

Nonrelativistic lattice study of stoponium

Seyong Kim*

*Department of Physics, Sejong University, Seoul 143-747, Korea and School of Physics,
Korea Institute for Advanced Study, Seoul 130-722, Korea
(Received 17 September 2015; published 5 November 2015)*

We calculate the bound state properties of stoponium using lattice formulation of nonrelativistic effective field theory for stop which is moving nonrelativistically in the rest frame of stoponium. Our calculation method is similar to that employed in lattice nonrelativistic quantum chromodynamics (NRQCD) studies for charmonium and bottomonium. Using $16^3 \times 256$ quenched lattice gauge field configurations at $a^{-1} = 50(1)$ GeV, we obtain the stoponium mass and the lattice matrix element which is related to the wave function at the origin for the $1S$ state and find that the lattice $|R_{1S}(0)|^2/M_{1S}^3$ is 3.5–4 larger than that from a potential model calculation for $200 \text{ GeV} \leq M_{1S} \leq 800 \text{ GeV}$.

DOI: 10.1103/PhysRevD.92.094505

PACS numbers: 12.38.Gc, 12.60.Jv, 14.40.Pq

I. INTRODUCTION

After the discovery of Higgs particle by ATLAS [1] and CMS [2] at LHC, detailed measurements of its property become very important and urgent. These precision measurements will open up a new opportunity to search for physics beyond the standard model. In particular, heavy particles which can decay into Higgs boson are under active experimental and theoretical investigations. Scalar top quark (stop), the supersymmetric partner of top quark and the next-to-lightest supersymmetric particle (NLSP), is one of such possibilities. Then, stoponia, bound states (binding through $SU(3)$ color gauge interaction) of stop and antistop may become interesting provided that stop is long-lived enough to form a bound state. They can serve as a probe to stop, and decay of stoponium via the stop–antistop pair annihilation into diboson states may be observed due to its distinct signature [3–7].

With regard to the production cross section calculation of stoponium, a next-to-leading order computation of the perturbative part of the production cross section is available [8,9] and a resummed next-to-next-to-leading logarithm calculation is performed [10]. Turning these perturbative calculations into phenomenological comparisons requires matrix elements for stoponium. With the observation that heavy quark moves slowly in the rest frame of quarkonium ($v^2 \sim 0.1$ in bottomonium and $v^3 \sim 0.3$ in charmonium where v is the heavy quark velocity in the rest frame of quarkonium), nonrelativistic quantum chromodynamics (NRQCD) is developed and the quarkonium production cross section is given in terms of perturbative parts and nonperturbative matrix elements [11]. Similarly, the parton-level differential cross section for the stoponium (Ψ) production in a collider can be given as

$$d\hat{\sigma}(ab \rightarrow \Psi + X) = \sum_n d\hat{\sigma}(ab \rightarrow \tilde{t}\tilde{t}[n] + X) \langle \mathcal{O}^\Psi[n] \rangle, \quad (1)$$

where a, b are partons, \tilde{t}, \tilde{t} are stop and antistop, n denotes the angular momentum of the stoponium states and $\mathcal{O}^\Psi[n]$ are generic forms of nonrelativistic stoponium production operators [8] by considering nonrelativistic effective field theory (NREFT) for stoponium system since in the rest frame of stoponium for $M \sim \mathcal{O}(100)$ GeV, v^2 is expected to be $\sim \mathcal{O}(0.01)$ and $\alpha_s(Mv) \sim \mathcal{O}(0.1)$.

Following [11], one can relate the production matrix elements to decay matrix elements by crossing relation in leading order of v^2 . The decay matrix elements then can be related to nonrelativistic wave functions in the vacuum saturation approximation up to $\mathcal{O}(v^4)$. For the $1S$ state stoponium,

$$\langle \mathcal{O}^\Psi \rangle \simeq \langle 0 | \chi^\dagger \psi | 1S \rangle \langle 1S | \psi^\dagger \chi | 0 \rangle = |\langle 0 | \chi^\dagger \psi | 1S \rangle|^2, \quad (2)$$

when the leading v^2 -order term in the factorization expansion is considered and a stoponium state is assumed to dominate in the intermediate states [11]. Here, ψ denotes nonrelativistic stop, χ^\dagger denotes nonrelativistic antistop. This matrix element is related to the wave function at the origin [11] as

$$|\langle 0 | \chi^\dagger \psi | 1S \rangle|^2 \simeq \frac{4\pi}{N_c} |R_{1S}(0)|^2 \quad (3)$$

and has been calculated on lattice for charmonium and bottomonium decays¹ [12–14] (see [15] for an improved lattice calculation for bottomonium system).

So far, potential model estimates (e.g., [16]) have been used for the stoponium masses and the stoponium wave functions where typical bound states properties are summarized in $\frac{|R_S(0)|^2}{M_S^3}$ with the mass of the S-wave stoponium

¹Note that in Eq. (3) the factor $\frac{1}{N_c}$ instead of $\frac{1}{2N_c}$, due to the spinless nature of stop.

*skim@sejong.ac.kr

state, M_S , and $|R_S(0)|$ the value of stoponium radial wave function at the origin. In $\frac{|R_S(0)|^2}{M_S^3}$, uncertainty from the wave function at the origin, $|R_S(0)|$, is more dominant than that from the mass. The mass of stoponium will be mostly from twice of the “free” stop mass and the “binding energy” will be just a few percent in stoponium mass and the uncertainty in binding energy will lead to subpercent level uncertainty in stoponium mass. On the other hand, $|R_S(0)|$ depends very much on the functional form of potential models [12,17,18].

Clearly, using potential model estimates for the binding interaction of stoponium is unsatisfactory since it introduces model-dependence which can not be systematically improved, and makes the stoponium cross section calculation unsystematic as a whole, despite the improved perturbative calculations. Furthermore, potential models have a difficulty in obtaining right decay widths for a given state although they do better for relative ratios for different states [17,18]. Employing different functional forms for potential models can lead to a large differences. For example, a potential model estimate for $|R_S(0)|$ defies a naive expectation that large stop mass ($M > 100$ GeV) would result in Coulombic behavior of the wave function, and exhibits substantial departure from the Coulombic value of $|R_S(0)|$ even at $M \approx 1$ TeV [16]. This suggests that there can be sizeable nonperturbative contribution to the bound state properties. Indeed, next-to-next-to-next-to-leading order calculation together with a scheme choice which is less sensitive to the long distance effect of QCD is necessary to understand the threshold behavior of the top antitop S-wave pair production cross section [19].

In this work, we use lattice formulation of v^2 NREFT for stoponium and calculate the stoponium mass and a stoponium matrix element, $|\langle 0 | \chi^\dagger \psi | \Psi \rangle|^2$. Unlike a potential model calculation, lattice NREFT is based on the first principles of quantum field theory and allows systematic study of errors associated with a given result. This effective lattice theory is similar to the lattice version of NRQCD [12,20] which allows highly successful understanding of nonperturbative quarkonium physics (see e.g., [15]) except for the fact that stop is a spinless particle. Our calculation for the stoponium property is performed on $N_s^3 \times N_\tau = 16^3 \times 256$ lattices generated with “quenched approximation” and the lattice spacing, $a^{-1} \approx 50$ GeV for the stop mass range $1 \leq Ma \leq 8$ (i.e., $50 \leq M \leq 400$ GeV). A large N_τ is necessary to avoid deconfining effects. In the rest frame of stoponium, stop is expected to move slowly with velocity $v (\ll 1)$ and the size of stoponium should be smaller than those of typical quarkonia [rough estimate for the size of stoponium may be given by the self-consistency relation, $v \sim \alpha_s(Mv)$ with the size of $r \sim (Mv)^{-1}$ and the stop mass M] and thus small N_s does not cause a significant finite volume effect. Since the momentum scale larger than the heavy particle mass is

“integrated out” in NREFT and Ma is chosen to be ~ 1 , we need to consider only the lattice spacing scale in lattice NREFT for stoponium.

We find that with $\mathcal{O}(v^2)$ NREFT Lagrangian, the lattice result for $|R_{1S}(0)|^2/M_{1S}^3$ is factor 3.5–4 larger than a potential model estimate in [16] for $200 \text{ GeV} \leq M_{1S} \leq 800 \text{ GeV}$. Although further study is necessary (in particular in view of the difficulty associated with quantifying the systematic uncertainty from the quenched approximation), this implies that the stoponium production rate at LHC may be larger than the current estimates based on the potential model. In the following, we briefly summarize the lattice method used in the calculation of stoponium properties (Sec. II). Then, we present our main result in Sec. III and conclude with Sec. IV.

II. METHOD

The effective Lagrangian for nonrelativistic stop in leading order of v^2 is given by

$$\mathcal{L} = \psi^\dagger \left(D_\tau - \frac{\mathbf{D}^2}{2M} \right) \psi + \chi^\dagger \left(D_\tau + \frac{\mathbf{D}^2}{2M} \right) \chi, \quad (4)$$

where ψ is a complex scalar field for stop which transforms as a $SU(3)$ vector and χ is that for antistop and D_τ (\mathbf{D}) are gauge covariant temporal (spatial) derivative under the strong interaction, $SU(3)$. Note that this leading order NREFT Lagrangian does not differ from that for NRQCD. The difference between stoponium NREFT Lagrangian and NRQCD Lagrangian occurs only when next-to-leading order NREFT Lagrangian is considered since the spin interaction (e.g., $\boldsymbol{\sigma} \cdot \mathbf{B}$) in NRQCD is $\mathcal{O}(v^4)$. Additional terms for NREFT Lagrangian in v^4 can be systematically studied by including

$$\begin{aligned} \delta\mathcal{L} = & -\frac{c_1}{8M^3} [\psi^\dagger (\mathbf{D}^2)^2 \psi - \chi^\dagger (\mathbf{D}^2)^2 \chi] \\ & + c_2 \frac{ig}{8M^2} [\psi^\dagger (\mathbf{D} \cdot \mathbf{E} - \mathbf{E} \cdot \mathbf{D}) \psi + \chi^\dagger (\mathbf{D} \cdot \mathbf{E} - \mathbf{E} \cdot \mathbf{D}) \chi]. \end{aligned}$$

As for the Monte Carlo data of $SU(3)$ lattice gauge fields which are used in the calculation, they are generated on $16^3 \times 256$ lattice in “quenched approximation” at lattice bare coupling $\beta = \frac{6}{g^2} = 8.751$ using a single plaquette Wilson action. Multihit Metropolis algorithm together with interleaving over-relaxation algorithm [21] is used for the gauge field update. Each configuration is separated by 1000 Monte Carlo sweeps. To convert a lattice result into a quantity in a physical unit, one needs a lattice spacing as a function of the bare coupling constant. In the scaling limit ($N_f = 0$ due to quenched approximation),

$$a\Lambda_L^0 = \exp\left(-\frac{1}{2b_0g^2}\right) (b_0g^2)^{-\frac{b_1}{2b_0^2}} = f(g) \rightarrow a^{-1} = \frac{\Lambda_L^0}{f(g)} \quad (5)$$

where $b_0 = \frac{11}{3} \frac{N_c}{16\pi^2}$ and $\frac{34}{3} (\frac{N_c}{16\pi^2})^2$. We use the light hadron spectrum calculation in [21] to set the lattice scale since the experimental value for $1P-1S$ level splitting is not available for stoponium. In [21], at $6/g^2 = 6.5$, $m_\rho(m_q \rightarrow 0)a = 0.200(4)$. We obtain $a^{-1} = 3.84(8)$ GeV ($\Lambda_L^0 = 5.10(1)$ MeV) from the lattice $m_\rho a$ and $m_\rho(\text{physical}) = 768.1(5)$ MeV. This scale setting introduces $\sim 2\%$ systematic error.² Thus, the scale for $\beta = 8.751$ is set as $a^{-1} = 50(1)$ GeV = $0.0039(1)$ fm.

Under the background of these lattice gauge field configurations, nonrelativistic stop correlators for $\mathcal{O}(v^2)$ are calculated using the evolution equation,

$$G(\mathbf{x}, \tau_0) = S(\mathbf{x}),$$

$$G(\mathbf{x}, \tau_i) = \left(1 - \frac{H_0}{2k}\right)^k U_4^\dagger(\mathbf{x}, \tau_{i-1}) \left(1 - \frac{H_0}{2k}\right)^k G(\mathbf{x}, \tau_{i-1}),$$
(6)

where $S(\mathbf{x})$ denotes an appropriate complex valued random point source, diagonal in $SU(3)$ color (random source improves the signal to noise ratio), and H_0 is the lattice Hamiltonian corresponding to Eq. (4) and $U_4(\mathbf{x}, \tau_{i-1})$ is the time directional gauge field. The parameter, k is introduced to stabilize large momentum behavior of the lattice discretized evolution equation (see Table I for the choice of k). The gauge link variables are divided by ‘‘tadpole factor’’, u_0 , which is chosen to be

$$u_0 = \langle 0 | \frac{1}{3} \text{Tr} U_{\text{plaq}} | 0 \rangle^{\frac{1}{4}}$$
(7)

where U_{plaq} is a plaquette. For $\mathcal{O}(v^4)$ Lagrangian, a modified evolution equation which includes the Hamiltonian for Eq. (5) together with the improvement term for finite lattice spacing [20] can be used such as

$$G(\mathbf{x}, \tau_0) = S(\mathbf{x}),$$

$$G(\mathbf{x}, \tau_1) = \left(1 - \frac{H_0}{2k}\right)^k U_4^\dagger(\mathbf{x}, 0) \left(1 - \frac{H_0}{2k}\right)^k G(\mathbf{x}, 0),$$

$$G(\mathbf{x}, \tau_i) = \left(1 - \frac{H_0}{2k}\right)^k U_4^\dagger(\mathbf{x}, \tau) \left(1 - \frac{H_0}{2k}\right)^k$$

$$\times (1 - \delta H) G(\mathbf{x}, \tau_{i-1}), \quad (i \geq 2),$$
(8)

where δH denotes the lattice v^4 Hamiltonian mentioned in the above.

²However, this small error bar should be taken with caution. The quenched approximation effect in the hadron spectrum can be as large as 20% and the ambiguity due to the quenched approximation in the scale setting is far larger. (see, e.g., [22] for the question of the scale setting in bottomonium system).

TABLE I. Mean field estimates of the zero energy shift.

Ma	k	ah_0	Z_M	$E_0 a$	$2(Z_M Ma - E_0 a)$
1.0	4	0.209385	1.04700	0.285172	1.52367
2.0	2	0.104926	1.04700	0.178845	3.83034
2.5	1	0.083941	1.03008	0.158271	4.83339
4.0	1	0.052463	1.04700	0.125682	8.12470
5.0	1	0.041971	1.05265	0.114935	10.2966
6.0	1	0.034975	1.05641	0.107803	12.4613
7.0	1	0.029979	1.05910	0.102724	14.6219
8.0	1	0.026232	1.06111	0.098923	16.7799

The zero-momentum stoponium correlators are then formed by combining the Green function for stop and that for antistop and are summed over the spatial lattice sites. From the stoponium correlators, matrix elements are obtained by fitting

$$G_S(\tau) = \sum_n e^{-E_n \tau} \langle 0 | \chi^\dagger \psi | n \rangle^2$$

$$= A_0 e^{-E_{1S} \tau} + A_1 e^{-E_{2S} \tau} + \dots$$
(9)

For the lattice determination of the wave-function at the origin, $|R(0)|^2$, the matrix element obtained from fitting Eq. (9) is related to the nonrelativistic Coulomb-gauge fixed wave-function

$$A_0 = |\langle 0 | \chi^\dagger \psi | 1S \rangle|^2$$
(10)

in the leading order of v^2 with the normalization convention for the radial wave function, $\int_0^\infty dr r^2 |R(r)|^2 = 1$ [11,12].

In NREFT formulation, the energy scale in the spectrum is not known. In order to determine the mass of a state from the energy of state for a given channel from Eq. (9), ‘‘energy shift’’ needs to be determined,

$$M_N = 2(Z_M M - E_0) + E_N$$
(11)

where the mass of state, M_N (N denotes the quantum number of the state), is given in term of the energy of the state (E_n), ‘‘zero point energy (E_0)’’, and the mass renormalization ($Z_M M$) [23] (or one can use the kinetic mass of nonrelativistic dispersion relation to determine the mass of a state [22]). In lattice NRQCD study of charmonium and bottomonium, this energy shift is determined either by the well measured experimental mass for one of the states (such as J/ψ and Υ) or by lattice perturbation theory computation [24]. Stoponium is not discovered yet and the perturbative estimate for the energy shift using the lattice action used in this work is not calculated. Thus, we use tadpole improved mean field estimate for the energy shift in leading order [20], where

$$E_0 = -a^{-1} \ln \left[u_0 \left(1 - \frac{ah_0}{2k} \right)^{2k} \right],$$

$$Z_M = u_0^{-1} \left(1 - \frac{ah_0}{2k} \right) \quad (12)$$

with

$$ah_0 = 3 \frac{(1 - u_0)}{Ma}. \quad (13)$$

n is the integer parameter which is introduced in Eq. (6) to prevent the high momentum instability of the evolution equation. At $\beta = 8.751$ ($g^2 = 1.4585$), Monte Carlo simulation gives $u_0 = 0.930049(1)$. Perturbatively, $u_0 \sim 1 - 0.083g^2 - \dots$ [20] and $u_0 \approx 0.94309$ at $\beta = 8.751$. The difference between the lattice value of u_0 and the perturbative value of u_0 is $\sim 1.4\%$, which suggests order of magnitude for nonperturbative effect in tadpole factor, u_0 at $\beta = 8.751$. Table I summarizes the mean field estimates of the energy shift for various Ma and n used for stoponium correlator calculation.

There are various sources for systematic errors with nonrelativistic lattice calculation of stoponium properties. An analysis similar to that in lattice NRQCD computation of quarkonium [20] can be applied: (i) relativistic correction, (ii) finite lattice spacing, (iii) radiative correction, (iv) finite lattice volume effect, and (v) light-quark vacuum polarization. In this work, there are additional sources of errors. First is the determination of the zero energy shift: due to the rest mass of the particle and its renormalization, NREFT has a undetermined “zero energy shift,” which can be fixed by an experimental mass of one of quarkonium states or by a perturbative calculation. Our use of a mean field theory approximation [20] for the shift introduces a source of systematic error. Additional error concerns a bare stop mass used in the lattice calculation. An accurate calculation of the stoponium masses requires “tuning of stop mass” which compares a stoponium kinetic mass in nonrelativistic dispersion relation for a given stop mass with an experimental stoponium mass and changes stop mass until the kinetic mass is equal to the experimental stoponium mass. Since stoponium is not discovered yet, this tuning procedure cannot be performed and the lattice result in the following contains an uncertainty from the imprecise tuning of stop mass.

III. RESULT

Figure 1 shows S-wave stoponium correlators, $G(\tau)$, on $16^3 \times 256$ lattice volume calculated with the v^2 Lagrangian [Eq. (4)] and the evolution Eq. (6) for each stop mass Ma , where the vertical axis is in the logarithmic scale. By fitting these stoponium correlators, we obtain the energy of 1S state, $E_{1S}a$ and the amplitude, A_0a^3 . Table II summarizes the fit results for each stop mass with the fit range

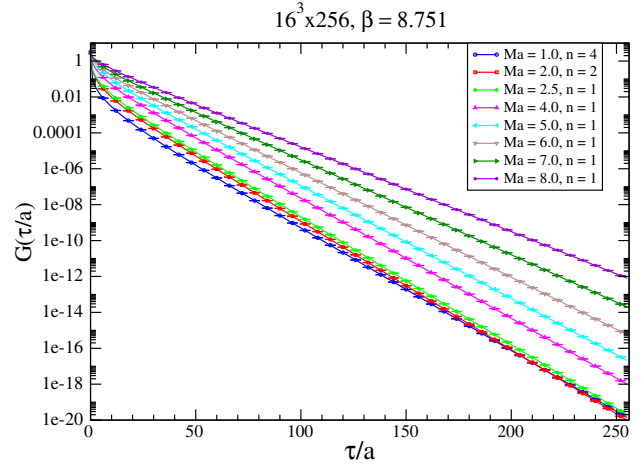


FIG. 1 (color online). The lattice nonrelativistic correlators for the S-wave channel with $\mathcal{O}(v^2)$ Lagrangian on $16^3 \times 256$ lattices.

$60 \leq \tau/a \leq 100$ where the fit range was chosen by locating the plateau region of the effective mass plot (Fig. 2). The error bar is from single elimination Jackknife error analysis of the fitted $E_{1S}a$ and A_0a^3 . From these lattice quantities, $E_{1S}a$ and A_0a^3 , we get M_{1S} and $|R_{1S}(0)|^2$ by use of Eq. (11) and Eq. (10) (the last two columns in Table II).

Figure 3 shows lattice $|R_{1S}(0)|^2/M_{1S}^3$ (the column 6 of Table II) as a function of lattice M_{1S} (the column 5 of Table II) in the range of $100 \text{ GeV} \leq M_{1S} \leq 800 \text{ GeV}$. In the figure, a line for a potential model result from [16] is also drawn for a comparison, where the $\Lambda = 300 \text{ MeV}$ parametrization for M_{1S} and $|R_{1S}(0)|^2/M_{1S}^3$ is used. The figure shows that the result from lattice NREFT calculation is larger by factor ~ 4 at $M_{1S} \sim 200 \text{ GeV}$ and by ~ 3.5 at $M_{1S} \sim 800 \text{ GeV}$ than that from a potential model calculation.

Let us consider the magnitude of the systematic errors in our lattice calculation of stoponium. First we consider the finite spacetime volume effect in Table II by comparing with the results from two different lattice volumes, Table III from $20^3 \times 256$ lattices and Table IV from $12^3 \times 256$

TABLE II. E_{1S} and A_0 from lattice calculation (in lattice unit) on $16^3 \times 256$ lattices with v^2 NREFT Lagrangian. The result is based on 400 stoponium correlators and the error bar is from the jackknife analysis of the 1-exponential fit.

Ma	k	$E_{1S}a$	A_0a^3	M_{1S} (GeV)	$ R(0) ^2/M_{1S}^3$
1.0	4	0.1619(2)	0.00507(4)	84.28(1)	$4.43(5) \times 10^{-3}$
2.0	2	0.1688(1)	0.02377(6)	200.0(1)	$1.557(7) \times 10^{-3}$
2.5	1	0.1671(1)	0.03599(7)	250.0(1)	$1.205(5) \times 10^{-3}$
4.0	1	0.1553(1)	0.1237(2)	414.0(1)	$9.13(3) \times 10^{-4}$
5.0	1	0.1455(1)	0.2353(3)	522.1(1)	$8.66(3) \times 10^{-4}$
6.0	1	0.1344(1)	0.4014(4)	629.8(1)	$8.41(3) \times 10^{-4}$
7.0	1	0.1220(1)	0.6173(5)	737.2(1)	$8.07(3) \times 10^{-4}$
8.0	1	0.1087(1)	0.8613(6)	844.4(1)	$7.49(3) \times 10^{-4}$

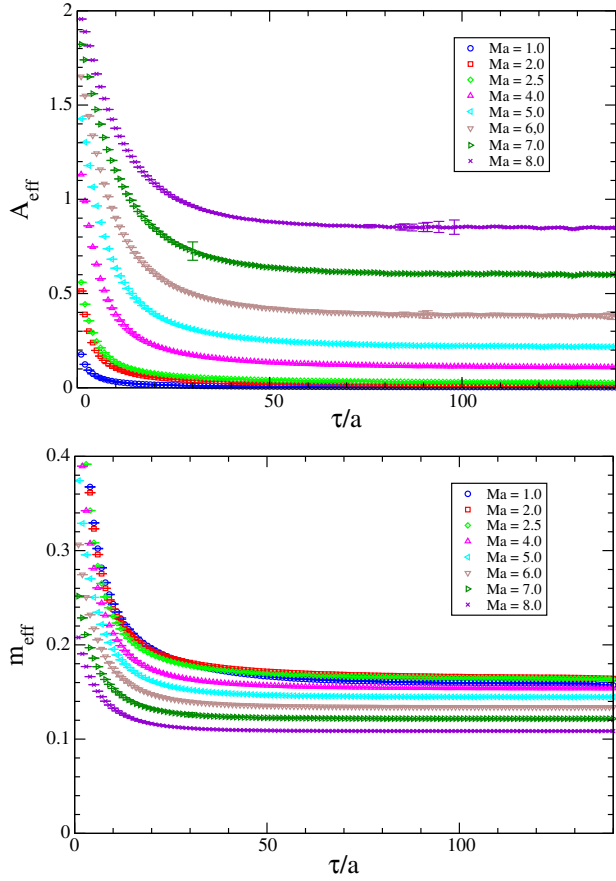


FIG. 2 (color online). The effective mass plot (bottom) and the A_0 plot (top) for the S-wave channel with $\mathcal{O}(v^2)$ Lagrangian using neighboring two points of the correlators ($G(\tau_i)$, $G(\tau_{i+1})$) on $16^3 \times 256$ lattices. Error bar is from Jackknife analysis.

lattices (both at $\beta = 8.751$ with the v^2 Lagrangian). These three tables show that between $16^3 \times 256$ and $20^3 \times 256$, there is little lattice volume dependence in M_{1S} and $|R_{1S}(0)|^2/M_{1S}^3$ but between $16^3 \times 256$ and $12^3 \times 256$, there

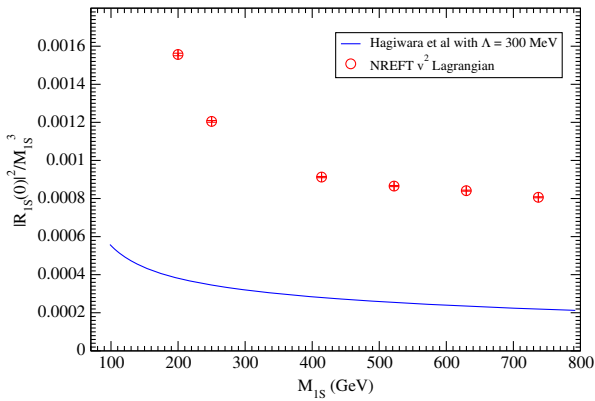


FIG. 3 (color online). $|R_{1S}(0)|^2/M_{1S}^3$ from nonrelativistic correlators for the S-wave channel on a $16^3 \times 256$ lattice with $\mathcal{O}(v^2)$ Lagrangian.

TABLE III. E_{1S} and A_0 from lattice calculation (in lattice unit) on $20^3 \times 256$ lattices with v^2 NREFT Lagrangian. The result is based on 400 stoponium correlators and the error bar is from the jackknife analysis of the 1-exponential fit.

Ma	k	$E_{1S}a$	$A_0 a^3$	M_{1S} (GeV)	$ R(0) ^2/M_{1S}^3$
1.0	4	0.1622(1)	0.00483(1)	84.29(1)	$4.22(1) \times 10^{-3}$
2.0	2	0.1693(1)	0.02438(4)	200.0(1)	$1.596(5) \times 10^{-3}$
2.5	1	0.1672(1)	0.03630(6)	250.1(1)	$1.216(4) \times 10^{-3}$
4.0	1	0.1553(1)	0.1233(1)	414.0(1)	$9.09(2) \times 10^{-4}$
5.0	1	0.1455(1)	0.2346(1)	522.1(1)	$8.63(3) \times 10^{-4}$
6.0	1	0.1343(1)	0.4007(3)	629.8(1)	$8.40(3) \times 10^{-4}$
7.0	1	0.1220(1)	0.6171(3)	737.2(1)	$8.07(2) \times 10^{-4}$
8.0	1	0.1087(1)	0.8617(4)	844.4(1)	$7.49(2) \times 10^{-4}$

TABLE IV. E_{1S} and A_0 from lattice calculation (in lattice unit) on $12^3 \times 256$ lattices with v^2 NREFT Lagrangian. The result is based on 400 stoponium correlators and the error bar is from the jackknife analysis of the 1-exponential fit.

Ma	k	$E_{1S}a$	$A_0 a^3$	M_{1S} (GeV)	$ R(0) ^2/M_{1S}^3$
1.0	4	0.1526(4)	0.0048(4)	83.81(2)	$4.27(39) \times 10^{-3}$
2.0	2	0.1635(2)	0.0193(2)	199.7(1)	$1.27(2) \times 10^{-3}$
2.5	1	0.1638(1)	0.0310(2)	249.9(1)	$1.040(9) \times 10^{-3}$
4.0	1	0.1549(1)	0.1201(2)	414.0(1)	$8.86(3) \times 10^{-4}$
5.0	1	0.1455(1)	0.2328(4)	522.1(1)	$8.56(3) \times 10^{-4}$
6.0	1	0.1344(1)	0.3994(6)	629.8(1)	$8.37(3) \times 10^{-4}$
7.0	1	0.1220(1)	0.6155(8)	737.2(1)	$8.04(3) \times 10^{-4}$
8.0	1	0.1087(1)	0.8592(9)	844.4(1)	$7.47(3) \times 10^{-4}$

are some lattice volume dependences. For $Ma \geq 4.0$, results from two larger lattice volumes agree within error bar. For $Ma < 4.0$, M_{1S} shows no difference and $|R_{1S}(0)|^2/M_{1S}^3$ has $\sim 3\%$ difference between the two larger lattices. Thus, we can conclude that the finite volume effect is small in the result from $16^3 \times 256$ lattices.

As discussed, in this work stop mass is not tuned and a mean field estimate of the zero energy shift is used. These two aspects are related to each other since tuning amounts to changing lattice stop mass until the kinetic mass in the nonrelativistic dispersion relation is equal to the mass of the a given state where part of the “correct mass” is from the zero energy shift, $2(Z_M M - E_0)$. However, tuning stop mass imprecisely is not a big source of systematic error. For example, in a bottomonium study [25], the difference between a properly tuned bottom quark mass, $Ma = 2.92$ and a rough estimate, $Ma = 2.90$ (using $M_b = 4.65$ GeV [26] and the lattice spacing 0.1127 fm) is consistent compared with the accuracy of our calculation. From Table I, one observes that the mean field estimate for the mass renormalization effect is small ($Z_M - 1 \sim 0.05$) at $\beta = 8.751$ and the variation in $E_0 a$ due to change of Ma is ~ 0.02 for $Ma \leq 4.0$ and ~ 0.005 for $Ma > 4.0$.

Furthermore the difference between the leading order perturbative estimate for the tadpole factor u_0 and the Monte Carlo estimate is 1.4%. Thus, the mean field estimates themselves must be close to the perturbative estimates for each quantity.

NREFT Lagrangian is an infinite series expansion in v^2 which up to $\mathcal{O}(v^4)$ is given in Eq. (4) and Eq. (5). Each term other than the kinetic term³ [Eq. (4)] comes with effective couplings and radiative corrections to these coefficients gives series expansions of α_s as $1 + c_i^{(1)}\alpha_s + \mathcal{O}(\alpha_s^2)$ for c_i and are expected to be less than 10% since $\alpha_s(M) \sim \mathcal{O}(0.1)$ for $M > 100$ GeV. Similarly, the discretization error due to the finite lattice spacing must be small since the magnitude of the improvement terms which correct for the finite lattice spacing effect of the spatial derivative ($\alpha_s \frac{a^2 \sum_i p_i^4}{12M} / \frac{p^2}{M} \sim \alpha_s \frac{(Ma)^2 v^2}{12}$) and the temporal derivative ($\alpha_s \frac{a(\sum_i p_i^2)^2}{8kM^2} / \frac{p^2}{M} \sim \alpha_s \frac{Mav^2}{8k}$) are small.

Estimating effects of the quenched approximation on the matrix element is difficult. In the bottomonium case, the comparison of S-wave function at the origin from the dynamical simulation [14] and that from the quenched simulation [13] using leading order NRQCD Lagrangian found that the matrix element from the quenched approximation underestimates by $\sim 40\%$ since the distance scale associated with the bottomonium bound state ($\sim \frac{1}{M_b v}$) is larger than the scale at which the matrix elements sample the wave function ($\sim a = \frac{1}{M_b}$).

In the lattice calculation of the matrix elements, the factorization scale is related to the lattice cutoff and the effective cutoff is affected by the specific form of the lattice action and the evolution equation of lattice Green's functions [27]. Such an effect needs to be studied if we are interested in the lattice matrix elements beyond the leading order of nonrelativistic expansion. Also, since the matrix element in Table II is actually a lattice matrix element, one needs to calculate perturbative matching coefficients between the lattice regularization scheme and a continuum regularization scheme which is used for the parton level cross section (e.g., $\overline{\text{MS}}$) to obtain continuum matrix elements. In this leading order NREFT Lagrangian study, the matching is not performed. However, since α_s is small, we expect that the renormalization effect will be small.

IV. SUMMARY

Under the assumption that stop is long-lived enough to form bound states, stoponium plays an important role in the study of stop and offers an interesting probe to stop searches [6,7]. In this case, nonperturbative quantity,

³In this case, tuning of the mass can absorb such correction (reparametrization invariance).

$|R_{1S}(0)|^2/M_{1S}^3$ where M_{1S} is the mass of 1S state of stoponium and $R_{1S}(0)$ is the radial part of the wave function at the origin, naturally appear in the study of productions and decays of stoponium. Thus far, a potential model estimate for $|R_{1S}(0)|^2/M_{1S}^3$ is used in phenomenological investigations of stoponium, which is unsuitable for improved perturbative calculations.

In this work, using lattice nonrelativistic formulation for heavy stop which is interacting through the strong interaction, we calculate the mass of S-wave stoponium and the stoponium matrix element relevant for stop-antistop annihilation decay, where this matrix element is related to $|R_{1S}(0)|^2$ in NREFT scheme. Compared to potential model studies, lattice study of stoponium is advantageous in that a particular functional form of the potential between stop and antistop needs not be assumed and errors associated with a lattice calculation can be systematically studied and improved.

Monte Carlo samples of $SU(3)$ color gauge field at $\beta = 8.751$ ($a^{-1} = 50$ GeV) on $16^3 \times 256$ lattices (which is generated in quenched approximation with multihit Metropolis/over-relaxation algorithm) is used for lattice calculation. Table II and Fig. 3 summarizes the lattice result for the 1S stoponium mass and the lattice matrix element for $|R_{1S}(0)|^2/M_{1S}^3$ with $\mathcal{O}(v^2)$ NREFT Lagrangian. In general, the lattice $|R_{1S}(0)|^2/M_{1S}^3$ is factor 3.5–4 larger than a potential model estimate of [16] for $200 \leq M_{1S} \leq 800$ GeV. The difference between the lattice result and the potential model result is larger at lighter M_{1S} and becomes smaller at heavier M_{1S} . According to this trend, the lattice result may approach Coulombic behavior of the wave function at heavier $M_{1S} > 1$ TeV although up to ~ 800 GeV the lattice result is still far from reaching Coulombic limit. E_{1S} , the energy of 1S state of stoponium ranges from ~ 6 GeV ($Ma = 1$) to ~ 8 GeV ($Ma = 8$). Up to v^2 order, toponium is equivalent to stoponium except the spin degeneracy and the result in Table II is equally applicable to toponium since the spin-flip term in NRQCD is $\mathcal{O}(v^4)$ [11].

Although further studies on systematic effects in our lattice result is necessary, factor 3.5–4 larger $|R_{1S}(0)|^2/M_{1S}^3$ implies an enhanced stoponium production cross section in hadron colliders such as LHC and can have interesting consequences for stop search in hadron colliders. Therefore, we hope to study stoponium using $SU(3)$ lattice gauge fields which includes vacuum polarization effect of light dynamical quark and improve the above result using $\mathcal{O}(v^4)$ NREFT Lagrangian in the future. For a next-to-leading order NREFT Lagrangian study, other matrix elements which are higher order in v^2 is also needed and the perturbative matching mentioned in the above needs to be performed. Since excited states of S-wave stoponium will contribute to the production cross section, matrix elements for excited states will be also interesting to study.

ACKNOWLEDGMENTS

We would like to thank C. T. H. Davies, R. R. Horgan for discussion during Royal Society International Scientific Seminars at Chicheley Hall, “Heavy quarks: a continuing probe of the strong interaction.” Discussions with Sunghoon Jung, Pyungwon Ko on stoponium

and Chaehyun Yu, Jungil Lee on quarkonium were helpful. This work is supported by the National Research Foundation of Korea funded by the Korean government (MEST) No. 2015R1A2A2A01005916 and in part by NRF-2008-000458.

-
- [1] G. Aad *et al.* (ATLAS Collaboration), Observation of a new particle in the search for the standard model Higgs boson with the ATLAS detector at the LHC, *Phys. Lett. B* **716**, 1 (2012).
- [2] S. Chatrchyan *et al.* (CMS Collaboration), Observation of a new boson at a mass of 125 GeV with the CMS experiment at the LHC, *Phys. Lett. B* **716**, 30 (2012).
- [3] M. Drees and M. M. Nojiri, A new signal for scalar top bound state production, *Phys. Rev. Lett.* **72**, 2324 (1994).
- [4] M. Drees and M. M. Nojiri, Production and decay of scalar stoponium bound states, *Phys. Rev. D* **49**, 4595 (1994).
- [5] S. P. Martin, Diphoton decays of stoponium at the Large Hadron Collider, *Phys. Rev. D* **77**, 075002 (2008).
- [6] N. Kumar and S. P. Martin, LHC search for di-Higgs decays of stoponium and other scalars in events with two photons and two bottom jets, *Phys. Rev. D* **90**, 055007 (2014).
- [7] B. Batell and S. Jung, Probing light stops with stoponium, *J. High Energy Phys.* **07** (2015) 061.
- [8] J. E. Younkin and S. P. Martin, QCD corrections to stoponium production at hadron colliders, *Phys. Rev. D* **81**, 055006 (2010).
- [9] S. P. Martin and J. E. Younkin, Radiative corrections to stoponium annihilation decays, *Phys. Rev. D* **80**, 035026 (2009).
- [10] C. Kim, A. Idilbi, T. Mehen, and Y. W. Yoon, Production of stoponium at the LHC, *Phys. Rev. D* **89**, 075010 (2014).
- [11] G. T. Bodwin, E. Braaten, and G. P. Lepage, Rigorous QCD analysis of inclusive annihilation and production of heavy quarkonium, *Phys. Rev. D* **51**, 1125 (1995); **55**, 5853 (1997).
- [12] B. A. Thacker and G. P. Lepage, Heavy quark bound states in lattice QCD, *Phys. Rev. D* **43**, 196 (1991).
- [13] G. T. Bodwin, D. K. Sinclair, and S. Kim, Quarkonium Decay Matrix Elements from Quenched Lattice QCD, *Phys. Rev. Lett.* **77**, 2376 (1996).
- [14] G. T. Bodwin, D. K. Sinclair, and S. Kim, Bottomonium decay matrix elements from lattice QCD with two light quarks, *Phys. Rev. D* **65**, 054504 (2002).
- [15] B. Colquhoun, R. J. Dowdall, C. T. H. Davies, K. Hornbostel, and G. P. Lepage, Υ and Υ' leptonic widths, a_μ^b and m_b from full lattice QCD, *Phys. Rev. D* **91**, 074514 (2015).
- [16] K. Hagiwara, K. Kato, A. D. Martin, and C. K. Ng, Properties of heavy quarkonia and related states, *Nucl. Phys.* **B344**, 1 (1990).
- [17] E. Eichten, K. Gottfried, T. Kinoshita, K. D. Lane, and T. M. Yan, Charmonium: Comparison with experiment, *Phys. Rev. D* **21**, 203 (1980).
- [18] W. Kwong, J. L. Rosner, and C. Quigg, Heavy quark systems, *Annu. Rev. Nucl. Part. Sci.* **37**, 325 (1987).
- [19] M. Beneke, Y. Kiyo, P. Marquard, A. Penin, J. Piclum, and M. Steinhauser, Next-to-next-to-next-to-leading order QCD prediction for the top anti-top S-wave pair production cross section near threshold in e^+e^- annihilation, [arXiv: 1506.06864](https://arxiv.org/abs/1506.06864).
- [20] G. P. Lepage, L. Magnea, C. Nakhleh, U. Magnea, and K. Hornbostel, Improved nonrelativistic QCD for heavy quark physics, *Phys. Rev. D* **46**, 4052 (1992).
- [21] S. Kim and D. K. Sinclair, The light hadron spectrum of quenched QCD on a $32 \times 3 \times 64$ lattice, *Phys. Rev. D* **48**, 4408 (1993).
- [22] A. Gray, I. Allison, C. T. H. Davies, E. Gulez, G. P. Lepage, J. Shigemitsu, and M. Wingate (HPQCD/UKQCD), The Upsilon spectrum and $m(b)$ from full lattice QCD, *Phys. Rev. D* **72**, 094507 (2005).
- [23] C. T. H. Davies, K. Hornbostel, A. Langnau, G. P. Lepage, A. Lidsey, J. Shigemitsu, and J. H. Sloan, Precision Upsilon spectroscopy from nonrelativistic lattice QCD, *Phys. Rev. D* **50**, 6963 (1994).
- [24] A. J. Lee, C. J. Monahan, R. R. Horgan, C. T. H. Davies, R. J. Dowdall, and J. Koponen, Mass of the b quark from lattice NRQCD and lattice perturbation theory, *Phys. Rev. D* **87**, 074018 (2013).
- [25] G. Aarts, C. Allton, T. Harris, S. Kim, M. P. Lombardo, S. M. Ryan, and J. I. Skullerud, The bottomonium spectrum at finite temperature from $N_f = 2 + 1$ lattice QCD, *J. High Energy Phys.* **07** (2014) 097.
- [26] J. Beringer *et al.* (Particle Data Group Collaboration), Review of particle physics (RPP), *Phys. Rev. D* **86**, 010001 (2012).
- [27] G. T. Bodwin, J. Lee, and D. K. Sinclair, Spin correlations and velocity-scaling in color-octet NRQCD matrix elements, *Phys. Rev. D* **72**, 014009 (2005).